Available online at www.sciencedirect.com

ScienceDirect

Procedia Manufacturing 10 (2017) 319 – 328

Procedia MANUFACTURING

45th SME North American Manufacturing Research Conference, NAMRC 45, LA, USA

Dynamic detection of instability defects in tube rotary draw bending

Enrico Simonetto[a,*],Andrea Ghiotti[a],Stefania Bruschi[a],Roberto Gemignani[b]

[a]*University of Padua, Department of Industrial Engineering, Padova 35131, Italy*
[b]*BLM Group S.p.a, Cantù 22063, CO, Italy*

Abstract

Tube rotary draw bending is commonly used to manufacture complex shaped elements in a wide range of geometries and applications. When thin-walled tubes are formed with small bending radii, the components may suffer of wrinkling at the intrados due to the critical process parameters. Off-line optimization approaches, which aim at predicting the correct process parameters and tool geometries, often require accurate data of the workpieces properties or the application of numerical simulation analyses, that may fail due to the scatter of such properties along the production batches. Therefore, the availability of on-line approaches to provide an adaptive response of the machine is crucial for the efficiency of highly automated production lines.
The paper presents the investigations carried out to assess the capability of dynamic analysis techniques to detect the instability defects that may affect the tubes in critical operating conditions. A new experimental approach, based on the analysis of dynamic data from the machine, is presented, as well as the evaluation of its performances when applied to the industrial process. The proposed approach appears promising for the detection of wrinkling, once they appear on the tube, and capable to give accurate feedback for the fast adjustment of the process parameters.

Peer-review under responsibility of the organizing committee of the 45th SME North American Manufacturing Research Conference

Keywords: tube bending, rotary draw bending, wrinkling, vibrations

* Corresponding author. Tel.: +39 049 8276816.
E-mail address: enrico.simonetto.1@phd.unipd.it

Peer-review under responsibility of the organizing committee of the 45th SME North American Manufacturing Research Conference
doi:10.1016/j.promfg.2017.07.064

1. Introduction

As consequence of the higher and higher demand of weight reduction in automotive, aviation and aerospace sectors, the deformation of thin-walled tubular components has become of major interest due to the extremely high stiffness-to-weight ratio that they present. However, the tube instability due to the compressive stresses at the intrados may cause wrinkling that makes the components not acceptable and affects dramatically the service life of the bending tools. Being dependent non only on geometric and material instabilities, but also on the process operating conditions (i.e. process temperature, interface conditions, tools pressure and, particularly, by the bending radius [1,2]), such defects are particularly difficult to be predicted and make critical the choice of the most proper process parameters to obtain sound components. At industrial level, the optimal set up of the process requires long-term experienced technicians and repeated trial-and-errors that are expensive, time consuming, and do not allow to predict eventual deviations of the process.

The problem of predicting instability defects has been approached by many researchers both analytically and numerically, being the latter methods more suitable to accurately reproduce the complex phenomena that involve the material and the contacts in the process, and the contributions can be generally grouped as (i) the static equilibrium method, (ii) the energy method, and (iii) the initial geometric imperfection method. The former addresses the problem using boundary condition equations, which allow the solution of the partial differential equilibrium equations [3] providing a general formulation of the wrinkling phenomenon as function of the specific individual parameters. Unfortunately, the more complex the boundary conditions or the geometrical shapes are, the more difficult the solutions become and the system of equation become impossible to be solved analytically. The second method aims at identifying the critical compressive stress states using the internal energy of the buckled component and the work done, under the hypothesis that the component can be considered in a stable equilibrium condition if the energy assumed for a deflection remains larger than the work given by the applied forces [4]. So, it allows avoiding the solution of the partial differential equilibrium equations, taking into account only the beginning and the end of the deformation by means of the deformation energy and the work force. The latter method moved from the observation that, when a cylindrical shell is experimentally compressed, the buckling takes place with loads as low as 30% of the theoretical ones due to initial geometric imperfection that characterize real tubes [5,6,7,8]. Although particularly attractive, the method appears difficult to be practically applied due to the complexity of the differential equations that have to be used in the description of the problem and the impossibility to accurate describe the initial imperfections that are usually idealized. As the geometric complexity of the application increases, numerical procedures based on Finite Element analyses are applied, where implicit or explicit algorithms appear the most suitable solutions in the case of large plastic deformations, rather than eigenvalue-base methods that are limited to deformations in the elastic field [9,10]. Unfortunately, all these methods appear sensitive to many input parameters, both numerical and experimental, and their calibration is extremely time consuming and expensive, making them not really effective when applied to real problems and poorly attractive to be implemented at industrial level.

With regard to the experimental investigations of the instability phenomena, the contributions are mainly limited to the post-processing of the defects to evaluate their entity [11] or for the calibration of the above mentioned approaches [12], but no researches were carried out with the objective of enable real-time controls of the process or corrections and/or reduction of the problem. The only researches carried out on the control of the tube bending process are limited and mainly directed at the springback evaluation by means of contact probes [13] or offline vision measurement systems [14].

The work presented in the paper is part of a research program that aims at developing real-time controls of the tube rotary draw bending processes, to prevent or correct the instability problems that can happens in critical operating conditions. The paper presents the investigations carried out to assess the capability of dynamic analysis techniques to detect the instability defects that may affect the tube intrados; in its first section it deals with the description of the industrial application case and the details of the investigated process conditions. The second part presents the new experimental approach, based on the analysis of dynamic data from the machine, as well as the evaluation of its performances when applied to the industrial process. Finally, the results of the measurements are presented.

2. Application case

2.1. CNC Rotary draw bending

The rotary draw bending process is performed on fully electric CNC machines, with a high production rate and accuracy. Figure 1 shows the main elements of the machine when positioned after the deformation: a straight tube is initially clamped by the clamping die and the bending die, which draw the tube section according to a predefined radius while rotating. A pressure die and a wiper die constrain the straight part of the tube, allowing a certain sliding of the tube during the drawing. The so called wiper die fills the gap between the tube and the bending die on the inner radius, to avoid the occurrence of wrinkles. The tube is supported internally by a mandrel that is made of a rigid body and a series of rotating ring joints to reduce the risk of collapsing the tube section and the wrinkling due to compressive stress states along the tube. A tie rod keeps the mandrel positioned during the bending and pull it out before the dies unloading. So, the process is stepwise, where the tube is manufactured in four consecutive stages, namely (i) clamping, (iii) bending, (iii) mandrel extraction, and (iv) unloading, and the tool motions are basically of transient type and temporally overlapped each other.

The process allows bending tubes even with very small curvature radii that can range between values of six times down to twice the outer diameter of the tube. Due to so low values of the curvature radii, high compressive stress states are introduced in the tube cross section, requiring an expert tuning of the process parameters to obtain sound components and, in particular, to avoid the problem of wrinkling. Among all, the most important parameters to be set concern the position and the force exerted by the pressure die to ensure the best contact between the tube and the wiper die on the inner tube bending diameter.

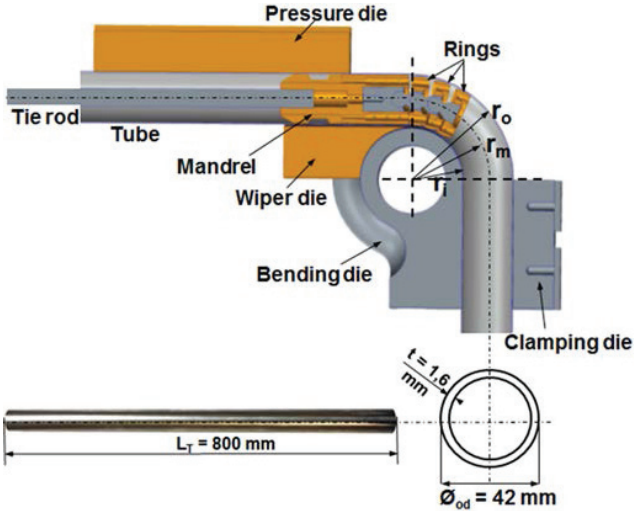

Fig. 1: Sketch of the cross section of the rotary draw bending dies, and main dimensions of the tube in the as-delivered conditions.

2.2. Material

The application case refers to an AISI 304 seam tube, with a length of 800.0(±0.5) mm, an outer diameter equal to 42(±0.1) mm and a thickness of 1.6(±0.1) mm, that is bent up to a maximum angle of 90 deg on a bending die having a nominal diameter of 120 mm. The CNC rotary draw bending machine is a fully electric BLM Elect 52™, see Figure 2, able to provide all data on the axis position, equipped with draw bending tools as shown in Figure 1. The bending die and the clamping die are made of 40NiCrMo7 steel, while the wiper die, the pressure die and the mandrel are made in a bronze alloy AMPCO M4 to avoid excessive wear due to the sliding with the tube inner walls. An inner mandrel with three ring joints was used in all the tests as in the industrial practice.

3. Experiments

3.1. Experimental equipment

Figure 2a shows the rotary draw bending machine used in the experiments, while the sensors that were applied for the investigation are shown in Figure 2b. Five Inertial Measurement Platforms (IMU), commercially available as MPU 6050 were used, each of them embeds three gyroscopes and three accelerometers to measure the accelerations and the angular speeds and has the maximum dimensions of 20x15x10 mm, including the printed circuit board and the wiring connection. The nominal measurement ranges are ±2 g for the accelerometers and ±250 deg/s in the case of the gyroscopes, with a 16-bit resolution per each single axis. The data acquired by the sensors are transmitted to an acquisition board using the Inter Integrated Circuit (I2C) protocol at an acquisition frequency of 600 Hz. The sensors have previously been calibrated and tested through the procedure already discussed in [15]. The IMUs were positioned on the main elements of the tooling set, namely the bending die B, the wiper die W, the mandrel M, the tie rod R, and on the tube T, to monitor the dynamic behaviour during the bending and the unloading stages, for a total number of 30 acquired signals, see Figure 2b. The sensors R and M, respectively mounted on the tie rod at a nominal distance of 3500 mm from the bending area and on the last ring joint of the mandrel, monitor the points of the structure closest to the deformation area [16]. The sensor T was fixed to the extremity of the tube that is bent and records the signal with the maximum intensity both in terms of vibrations and rotational speed, even if such position is suitable only for laboratory measurements and not for an industrial use. The sensor W, is the closest to the wrinkling area of the tube, while the sensor B is positioned on the top of the rotation die to monitor the behaviour of the engines as the instabilities appear. According to their positions, during the bending stage, M measure both translations and rotations, B and T respectively a rotational and a translational movement, while R and W do not detect any movement since they dies were they are mounted are fixed during the bending stage.

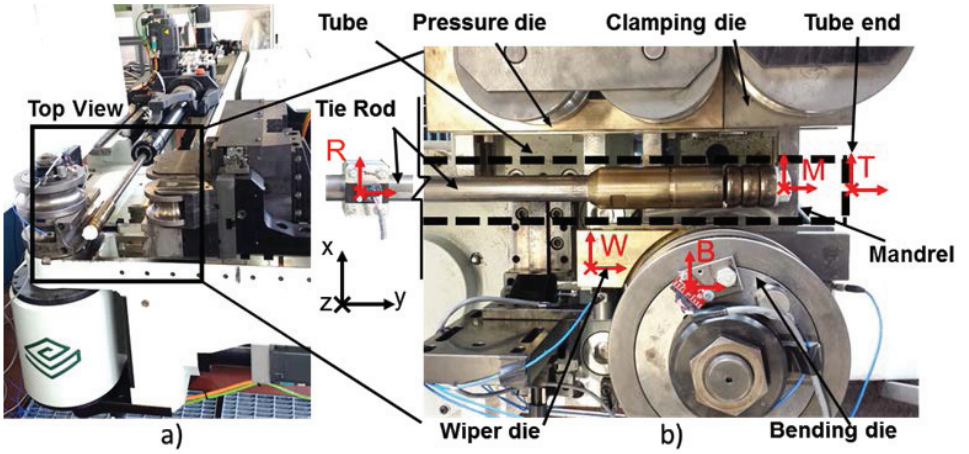

Fig. 2: a) front view of the bending machine; b) top view of the dies instrumented with the sensors.

Two additional piezoelectric uniaxial accelerometers (ICP® accelerometer – Model 353B33), with a sensitivity of 100 mV/g and sampled at frequencies up to 100kHz, were positioned at the measuring points B and W to investigate the presence of high frequency vibrations. To synchronize all the monitored data with the signals from the electric motors of the CNC machine, an algorithm in Matlab® environment that allows also the post processing of the data was developed.

3.2. Experimental plan

The experimental plan was carried out on the machine described in the section 2, equipped with the system shown in section 3.1. The tests were performed to investigate the influence of two parameters, namely the bending speed and the position of the pressure die. The latter allows obtaining the condition of sound component in the case

of correct positioning of the dies, named standard position, and the occurrence of wrinkles with an erroneous dies set up, named off-set position. In the former, the position of the pressure die is indicated with the value 0 as the reference case that return a sound component. The test conditions are summarized in Table 1, where each condition was repeated three times.

Table 1: Experimental plan

Parameter	Standard	Off-set
Bending angle[deg]	90	90
Bending die angular rater [deg/s]	13.2; 26.4	13.2; 26.4
Pressure die position [mm]	0	1.5

4. Results

4.1. Analysis in the time domain

Figure 3 shows the plot of the tools displacements and of the angular rate $\dot{\theta}_{zM}$ measured in the direction perpendicular to the bending plane by the sensor fixed on the mandrel (position M), respectively in the standard and off-set conditions. With regard to the angular rate, the four above mentioned process steps are shown in Figure 3, respectively:

i. *bending step*, in which the bending die and the clamping die rotate around the bending axis, while the articulated portion of the mandrel is free to rotate according to the tube deformation. According to the kinematic that was defined for motors (see dashed lines in Figure 3), the bending stage is carried out at constant angular rate in the time range between 0.5 s and 4 s. In the configuration standard, the signal of $\dot{\theta}_{zM}$ acquired at the point M shows a sudden increase at the beginning of the process up to a bent angle of 30 deg, that represents the maximum curvature angle that can be covered by a three-ring joints mandrel design. Differently, in the off-set case, the same sensor is sensitive to the vibrations due to the wrinkling at the tube intrados even for bending angles over 30 deg (in the time range between 2s and 4s), since its proximity to the area where the defects are produced.

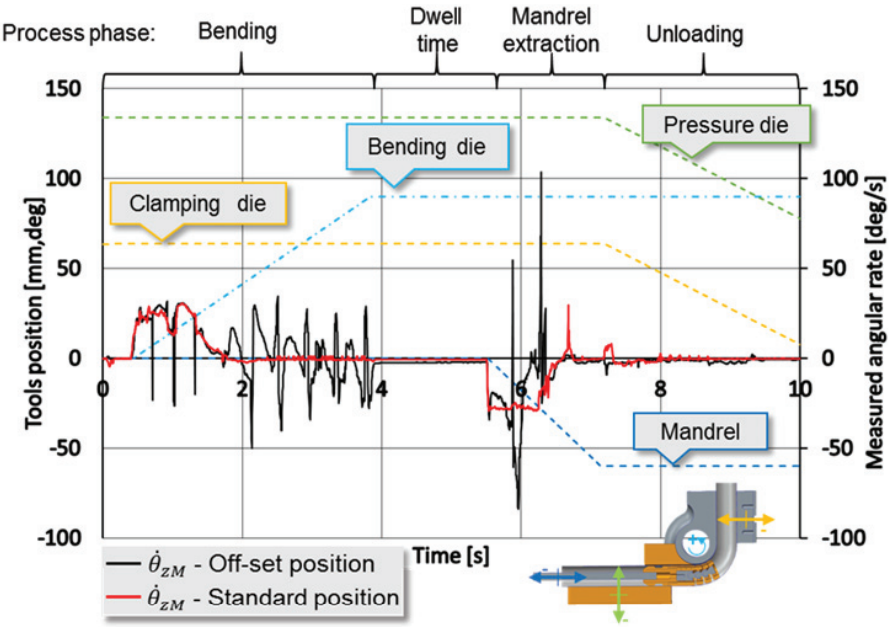

Fig. 3: plot of the tools displacement and of the angular rate measured at the position M in the standard and off-set conditions.

ii. *dwell time step*, between 4 s and 4.5 s that has been programmed after the previous step to allow the damping of the vibrations risen in the system.

iii. *mandrel extraction step*, during which the mandrel is pulled out from the rear side of the tube before the dies unloading. The angular velocity $\dot{\theta}_{zM}$ measured at this stage for the standard condition is opposite than the bending step due to the direction of rotation. Conversely, in the off-set case, several acceleration peaks can be noticed that are caused by the last defects appeared on the tube intrados, see Figure 6.

iv. *unloading step*, in which the clamping and pressure dies are opened and the tube unloaded.

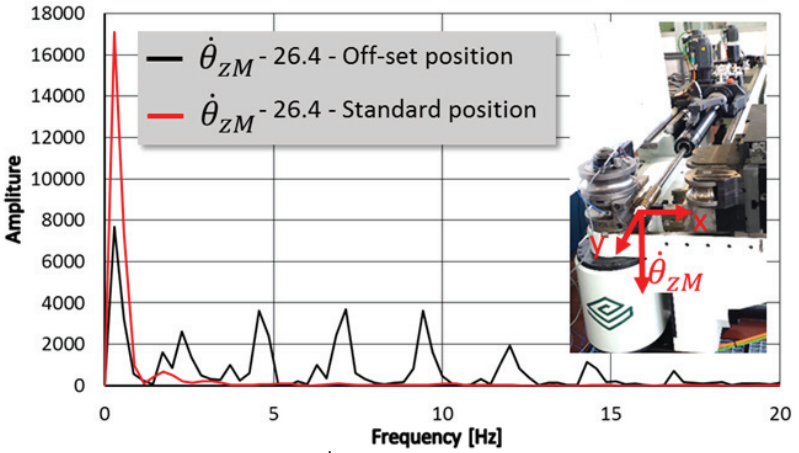

Fig. 4: spectrum of the angular rate $\dot{\theta}_{zM}$ at the point *M* in the standard and off-set conditions.

4.2. Analysis in the frequency domain

Table 2: Frequencies of the main peaks with an angular rate of 26.4 deg/s in the off-set condition.

Peak number	1	2	3	4	5
Peak frequency [Hz]	2.25	4.57	7.14	9.43	12

The analysis of the bending step in the frequency domain can allow a more accurate understanding of the instabilities that appear at the tube intrados when non appropriate process parameters are set. Figure 4 shows the spectrum of the angular speed $\dot{\theta}_{zM}$, measured by the sensor located at position M, while Table 2 reports the values of the frequencies peaks. Besides the initial peak at 0.28 Hz that is due to the choice of a sampling window of 3.6 s for the spectrum analysis, in the standard condition, in which the tube is bent without defects, no other peaks are detected during the bending step, while in the off-set position, in which the tube is bent without defects, the spectrum shows several peaks below 20 Hz that are equally spaced of about 2.4 Hz.

Figure 5 shows the frequency spectrum in the case of the off-set condition, acquired at the point M for two different levels of angular rate, respectively 13.2 deg/s and 26.4 deg/s. The results show that variations of the

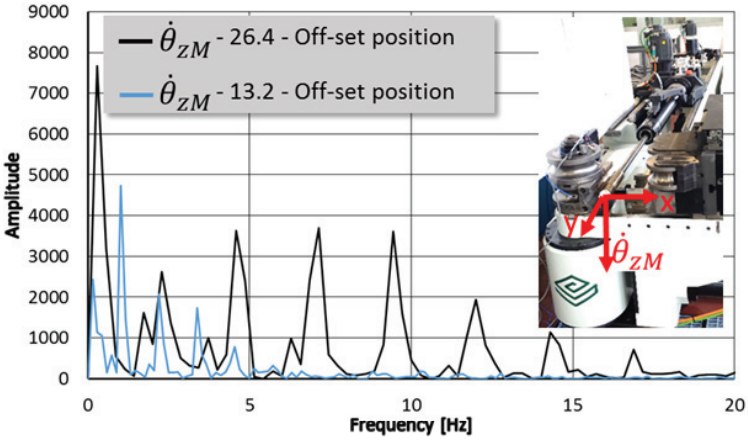

Fig. 5: spectrum of the signal at point *M* at different angular rates both in the off-set conditions.

bending velocities cause the shift of the measured peaks: the higher the angular rate of the process, the higher the frequencies at which the peaks are detected, while the distance between the peaks gets larger as the bending die angular rate increases, with an average distance between the peaks of 1.15 Hz and 2.4 Hz respectively. It can be noticed that also the number of peaks increases at higher angular rate: if the angular rate is doubled the induced vibrations are greater in magnitude leading to a higher number of harmonics detected. The values of the peaks detected for the lowest angular rate are reported in Table 3. Figure 6 shows the spectrum of the accelerations A_{XM} measured in the X direction, both in the standard and off-set conditions, for different values of angular rates. For the latter condition, at the angular rate of 26.4 deg/s, the peaks are equally spaced of 2.4 Hz, while at the lower angular rate of 13.2 deg/s the peaks are narrower distributed and do not allow an accurate identification of an average distance among them since the signal become comparable with the noise of the process.

Table 3: Frequencies of the main peaks with an angular rate of 13.2 deg/s in the off-set condition.

Peak number	1	2	3	4	5
Peak frequency [Hz]	1.03	2.20	3.37	4.54	5.72

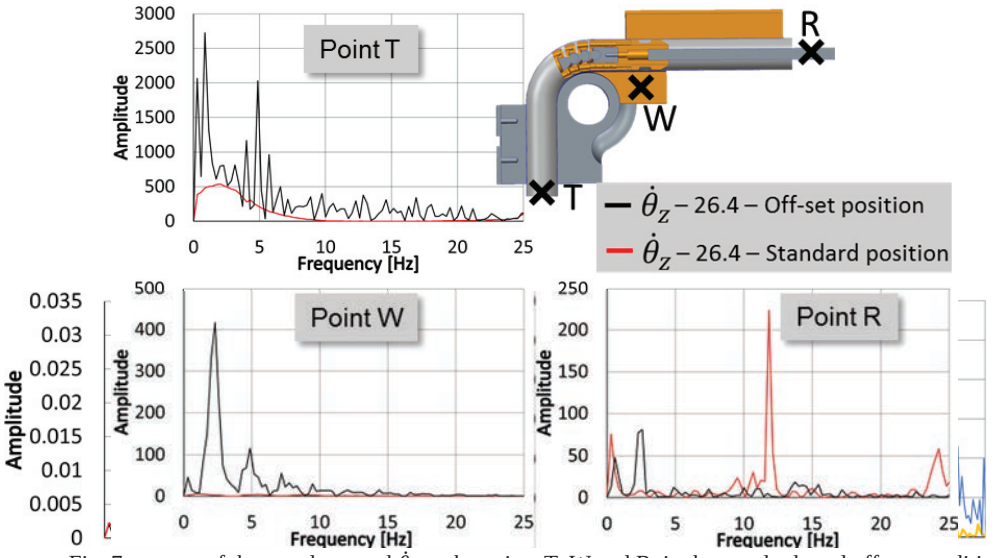

Fig. 7: spectra of the angular speed $\dot{\theta}_z$ at the points T, W and R, in the standards and off-set conditions.

Fig. 6 Spectra of the accelerations A_{XM} in the X-direction at the point M in the standard and off-set conditions.

Figure 7 shows the spectra of the angular rate along the Z axis, $\dot{\theta}_z$, measured at the positions T, W and R. The results show that the vibrations caused by the wrinkling are not high enough to have a relevant impact in all the areas of the machine. As example, the data recorded at the position R are weakly linked to the wrinkling, since only the shift of the main peak was detected by varying the testing conditions from the standard one. In the case of tube wrinkling, the signals measured at the point T present several peaks narrowly distributed, but with a poor correlation to the entity and the number of defects obtained on the tube. Only the spectrum obtained for the signals at the position W appears to be weakly linked to the vibration generated by the wrinkles as it is proved by the presence of several peaks that appear equally spaced with a period of 2.4 Hz, similarly to the values detected at the point M. The influence of the angular speed was detected as well, but in all the tests it was noticed that the only effect is the shift of the peaks directly proportional to the angular rate. The sensor fixed on the bending die (point B), it is not sensitive to vibration directly caused by the wrinkles.

4.1. Wrinkling analysis

Figure 8 shows a detail of the defects that were obtained on a bent tube. The experiments show that the distance between the peaks that was measured through the analyses in the frequency domain can be related to the gap between adjacent wrinkles Lw. In order to measure such distance, the bent tubes were cut in the longitudinal section and Lw was measured by means of optical analyses. Table 4 shows the value measured from the experimental tests. Such values can be explained by the fact that the gap between two wrinkles is influence by the mandrel shape and little sensitive to angular rate of the process.

Table 4: Wrinkling measurement in the experimental tests.

Condition	Standard		Off-set	
Angular rate [rad/s]	26.4	13.2	26.4	13.2

L_W [mm]	-	-	11.4±0.5	11.6±0.5
Nb. of Wrinkles	0	0	6	6

The angle α_w between two wrinkles can be calculated as:

$$\alpha_w = \frac{L_w}{r_i} = \frac{11.5}{60} = 0.192\ rad\ = 10.99\ deg \quad (1)$$

Considering the angular rate of the bending die $\dot{\theta}_{BD}$, the time period between two subsequent wrinkles Δt_w can be calculated using the equation 2:

$$\Delta t_w = \frac{\alpha_w}{\dot{\theta}_{BD}} \quad (2)$$

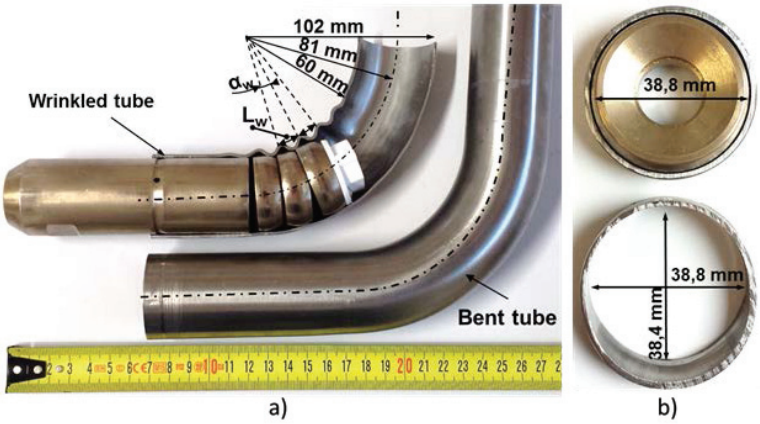

Fig. 8 a) bent tube, and wrinkled tube section with the mandrel positioned as at the end of the bending phase; b) front section of the tube in the not deformed zone (top) and in the wrinkles zone (bottom).

Being the periods Δt_w for the two tested condition respectively 0.41 s and 0.83 s, the wrinkles occur with a frequency of 2.4 Hz and 1.2 Hz, equal to the distance between the peaks in the spectra of the measured signals. So, the methodology appears effectiveness for the identification not only of the wrinkles, but also for the estimation of the wrinkles geometry obtained by non-proper set up of the tools.

These are prerequisites for the development of an automatic in-line adjustment method of the process parameters. A similar method, if wrinkles are identified, can operate a mandrel repositioning or an adjustment of the tools position proportional to the magnitude of the detected wrinkles.

5. Conclusions

The paper presents the investigations carried out to assess the capability of dynamic analysis techniques to detect the instability defects that may affect the tubes in critical operating conditions. A new experimental approach, based on the analysis of dynamic data from the machine, is presented, as well as the evaluation of its performances when applied to the industrial process. The experiments showed that the mandrel is the most sensitive element to detect the wrinkles that are produced during not properly set up bending processes. The wiper die appears also a suitable point to detect the wrinkling, although less sensitive if the defect is not evident. The analysis of the acquired signals in the frequency domain allowed to estimate the number of the defects that appeared on the tube intrados and the influence of the process angular rates. With regards to the latter, the higher the angular rate of the process, the higher the frequencies at which the peaks are detected, while the distance between the peaks gets larger as the bending die angular rate increases, with an average distance between the peaks of 1.15 Hz and 2.4 Hz respectively. The

geometrical analyses of the defects showed that the distance between the wrinkles can be related to the gap between two peaks of signal in the frequency domain. It was noticed that the gap between the wrinkles is not influenced by the dynamic conditions of the process, but it seems mainly related to the geometry of the tools. The system has been tested in conditions of severe wrinkles to identify which measurement points allow to identify their presence. The points identified will be monitored in further tests to evaluate the system and the analysis strategies in the case of less severe and more localized wrinkles.

Acknowledgements

The authors wish to thank the company BLM Group S.p.a. (Italy), for the support provided in the definition of the industrial case and in the activities carried out in the experimental plan.

References

[1] H. Yang, Y. Lin, Wrinkling analysis for forming limit of the tube bending processes. Journal of Material Processing Technology, 152 (2004) 363-369.
[2] L. Nan, H. Yang, L. Heng, Y. Siliang, Plastic wrinkling prediction in thin-walled part forming process: a review. Chinese Journal of Aeronautics, 19 (2016) 1-14.
[3] L. Shiqiang, F. Jun, W. Kelu, Plastic deformation analysis and forming quality prediction of tube NC bending. Chinese Journal of Aeronautics, 29 (2016) 1436-1444.
[4] G.Y. Zhao, Y.L. Liu, C.S. Dong, H. Yang, X.G. Fan, Analysis of wrinkling limit of rotary-draw bending process for thin-walled rectangular tube. Journal of Materials Processing Technology, 210 (2010) 1224-1231.
[5] A. Limam, L.H. Lee, S. Kyriakides. On the collapse of dented tubes under combined bending internal pressure. International Journal of Mechanical Sciences, 55 (2012) 1-12.
[6] H. Yang, J. Yan, M. Zhan, H. Li, Y. Kou, 3D numerical study on wrinkling characteristics in NC bending of aluminum alloy thin-walled tubes with large diameters under multi-die constraints. Computational Materials Science, 45 (2009) 1052-1067.
[7] A. Limam, H. Lee, E. Corona, S. Kyriakides, Inelastic wrinkling and collapse of tubes under combined bending and internal pressure. International Journal of Mechanical Sciences, 52 (2010) 637-647.
[8] L. Nan, H. Yang, L. Heng, T. Zhijun, H. Xiao, An imperfection-based perturbation method for plastic wrinkling prediction in tube bending under multi-die constraints. International Journal of Mechanical Sciences, 98 (2015) 178-194.
[9] G.Y. Zhao, Y.L. Liu, H. Yang, C.H. Lu, Cross-sectional distortion behaviors of thin-walled rectangular tube in rotary-draw bending process. Transaction of Nonferrous Metals Society of China, 20 (2010) 484-489.
[10] T. Wen, On a new concept of rotary draw bend-die adaptable for bending tubes with multiple outer diameters under non-mandrel condition. Journal of Material Processing Technology, 214 (2014) 311-317.
[11] T. Shan, L. Yuli, H. Yang, Effects of geometrical parameters on wrinkling of thin-walled rectangular aluminum alloy wave-guide tubes in rotary-draw bending. Chinese Journal of Aeronautics, 16 (2013) 242-248.
[12] L. Nan, H. Yang, L. Heng, M. Zhan, T. Zhijun, H. Xiao, Modelling of wrinkling in NC bending of thin-walled tubes with large diameters under multi-die constraints using hybrid method. 11th International Conference on Technology of Plasticity 2014, Procedia Engineering, 81 (2014) 2171-2176.
[13] J.M. Allwood, S.R. Duncan, J. Cao, P. Groche, G. Hirt, B. Kinsey, T. Kuboki, M. Liewald, A. Sterzing, A.E. Tekkaya, Closed-loop control of product properties in metal forming. CIRP Annals – Manufacturing Technology, 65 (2016) 573-596.
[14] S. Katona, M. Lušić, M. Koch, S. Wartzack, Integrating optical 3D measurement techniques in pipe bending: a model-based approach minimizing waste by deriving real functional design behaviour. Procedia CIRP, 50 (2016) 808-812.
[15] E. Simonetto, A. Ghiotti, S. Bruschi, Feasibility of motion-capture techniques applied to tube bending. Key Engineering Materials, 651-653 (2015) 1128-1133.
[16] A. Ghiotti, 2016, Apparatus for improving the quality of tube bending and method that uses such apparatus, (2016) patent nb. WO2016IB51833 20160331.